

# Communications to the Editor

## Evidence of a Novel Side Chain Structure in Regioregular Poly(3-alkylthiophenes)

T. J. Prosa and M. J. Winokur\*

Department of Physics, University of Wisconsin, Madison, Wisconsin 53706

R. D. McCullough

Department of Chemistry, Carnegie Mellon University, Pittsburgh, Pennsylvania 15213

Received October 11, 1995

Revised Manuscript Received February 23, 1996

Clarifying the changes in the physical behavior of flexible side chain substituted  $\pi$ -conjugated and other rodlike polymers continues to be an important research topic. For conducting polymers, this side chain addition, when coupled with controlled synthesis, has been shown to dramatically enhance key electronic properties and profoundly alter the macromolecular structures.<sup>1–4</sup> In particular, the ability to specify the extent of poly(3-alkylthiophene) (P3AT) chemical regularity,<sup>4–6</sup> with respect to side chain positioning, has increased the maximum observable conductivities as well as focused attention on the role that side chains play. Regioregular poly(3-dodecylthiophene) (R-P3DDT), with 98% head-to-tail (HT) coupling of the alkyl side chains along the backbone, has conductivities (when doped with an electron acceptor) up to 50 times those seen in the “regioirregular” counterpart (IR-P3DDT) having only 75% HT linkages. R-P3DDT, which contains a high proportion of insulating side chains, also exhibits conductivities up to twice those reported for the unsubstituted parent polymer, polythiophene. There are other surprising features as well. P3AT's are also found to be thermo- and solvatochromic.<sup>1,7</sup> Many P3AT samples exhibit semicrystalline lamellar phases exhibiting a thermotropic transition to a liquid crystalline (LC) state.<sup>8,9</sup> While these mesophases may improve processibility, they also have the potential for altering the electronic properties. Consequently, the full range of structure–property interrelationships that side chains impart to these polymers needs to be explored in order to realize their full potential and limitations.<sup>10</sup>

The most prevalent crystal structure reported for P3AT's has been studied extensively.<sup>8,9,11–13</sup> These studies support a lamellar base structure in which parallel stacks of polymer main chains are separated by regions filled by the alkyl side chains (see inset of Figure 1). Each layer consists of stacked arrays of the main chains spaced 3.8 Å apart and sequentially displaced, along the skeletal *c*-axis direction, by one thiophene unit (*d*/2 or 3.9 Å), resulting in a staggered nesting of the side chains. Structure factor intensity calculations<sup>9</sup> support a model in which these side chains are strongly tilted at an angle such that this side chain nesting approximates a 4.5 Å hexagonal close packing in close correspondence to the average packing of pure alkanes or polyethylene.<sup>14</sup> Overlap (interdigitation) between side chains in neighboring stacks is minimal although there can be ordering of the side chains across

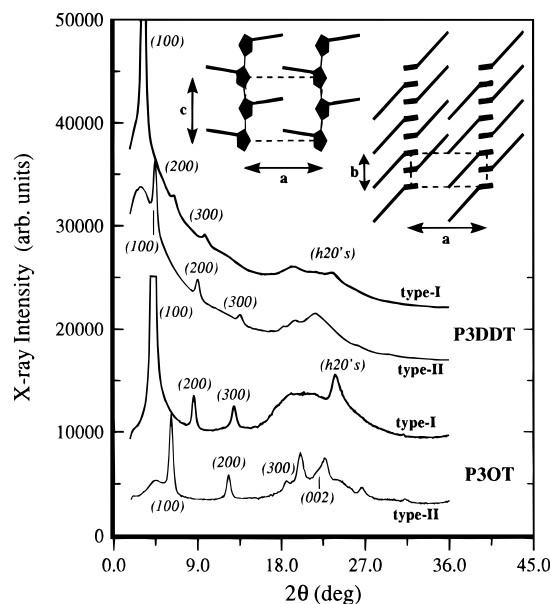


**Figure 1.** Typical X-ray powder diffraction profiles of P3DDT and P3OT for type-I and type-II crystal structures. Inset: Schematic model of the type-I crystal structure.

the layer–layer interface.<sup>9</sup> Additional phases are described<sup>15–18</sup> but the full structural details are incomplete.

In this communication we elucidate the fundamental side chain organization within a novel<sup>19</sup> P3AT crystal phase that forms during solvent casting from *m*-xylene of both regioregular P3AT samples studied, R-P3DDT and R-P3OT, i.e. poly(3-octylthiophene). This lamellar phase is found to incorporate a complete interlayer interdigitation of the side chains, and good agreement of the crystalline phase peak positions *and* intensities is obtained using this fully interdigitated (ID) model. This X-ray data cannot be satisfactorily reproduced using a non-ID structure. Depending on the casting conditions, films having either an ID or non-ID structure may form. Furthermore, modest heating of the ID phase initiates a rapid (and nominally irreversible<sup>20</sup>) solid-state transformation to the familiar, non-ID structure typically seen in both IR- and R-P3AT's.

The P3AT samples used were synthesized by polymerization of 2-bromo-5-(bromomagnesio)-2-alkylthiophene using catalytic amounts of Ni(dppp)Cl<sub>2</sub>.<sup>21</sup> The final polymer has essentially uniform regiochemical HT coupling when compared to polymers synthesized by direct oxidative coupling methods.<sup>1</sup> R-P3OT and R-P3DDT films were formed by evaporation in air of 1–3% (by weight) polymer/*m*-xylene solutions onto thin mica sheets at both room temperature (*T<sub>R</sub>*) and ca. 60 °C. The samples cast at 60 °C formed in 1–3 h and resulted in a blackish, shiny, flexible film (type-I). The *T<sub>R</sub>* films were obtained by first heating the polymer/*m*-xylene mixture until the polymer completely dissolved and then cooling. These samples required from 1 to 2 days to form and gave a very different appearance. As the solvent evaporated, a swollen gel-like phase first ap-

peared and shrank. As the residual solvent left, the "films" broke apart into a large number of smaller flaky pieces (type-II) which were dark and brittle.

The X-ray instrumentation consisted of a rotating anode generator, a copper target ( $\lambda_{K\alpha} = 1.542 \text{ \AA}$ ), an elastically bent LiF monochromator, a  $120^\circ$  ( $2\theta$ ) curved wire detector ( $0.1^\circ$  resolution), and He beam paths. The polymer samples were mounted in transmission geometry. For thermal studies, samples were placed in a heater cell stabilized to better than  $\pm 2^\circ \text{C}$ . Acquisition times varied from 1 to 4 h, with typically  $2 \times 10^7$  counts recorded across the entire detector array.

Example powder diffraction spectra for P3AT type-I and type-II structures are shown in Figure 1. These type-I profiles are equivalent to those reported previously. This "typical" pattern has the telltale sequence of evenly spaced low-angle reflections [(100), (200), etc.] indicative of the 20.8 and 27.1  $\text{\AA}$  lamellar interlayer spacing for R-P3OT and R-P3DDT, respectively. In addition, there is a "single"<sup>9</sup> wide-angle peak located near  $2\theta = 24^\circ$  dominated by scattering identified with the intrastack chain-to-chain repeat of  $\sim 3.8 \text{ \AA}$ . This latter feature is superimposed on a broad amorphous halo centered near  $2\theta = 20.5^\circ$  (or a 4.3  $\text{\AA}$  "d-spacing") which has been attributed to side chain disorder. The type-II profiles, once again, exhibit a series of evenly spaced low-angle peaks but their positions are strongly shifted to much higher angles implying a  $\sim 30\%$  reduction in the interlayer repeat to 14.5 and 19.8  $\text{\AA}$  for R-P3OT and R-P3DDT, respectively. Furthermore, there are a number of new peaks present in the  $2\theta = 18\text{--}30^\circ$  region. The strongest of these occurs at  $2\theta = 19.9^\circ$  and nominally implies an intrastack d-spacing of 4.47  $\text{\AA}$ . Finally, the amorphous halo now appears centered about a higher  $2\theta$  angle of  $22.5^\circ$  (or 3.9  $\text{\AA}$ ).

The large average unit cell dimensions, powder averaging, and small number of individually resolved Bragg-like reflections limit the efficacy of a simple peak indexing and the overall convincingness of a quoted structure. In order to further validate a model's suitability, we simultaneously calculated the scattering intensities of template structures using the methods of ref 9. The structural model best able to reproduce both peak positions and intensities (shown by the comparison spectra of Figure 2) has the side chains from neighboring main chain stacks fully interpenetrating as shown in the Figure 2 inset. The base P3OT model<sup>22</sup> for this comparison uses a two polymer chain unit cell ( $a = 15.3 \text{ \AA}$ ,  $b = 9.43 \text{ \AA}$ ,  $c = 8.07 \text{ \AA}$ , and  $\gamma = 72^\circ$ ) employing a *trans*-planar polythiophene skeleton consisting of 100% HT-HT couplings in combination with an all-*trans* side chain conformation. The average orientation of the linear side chains is controlled by varying the bond and dihedral angles across the C-C linkage which anchors the side chain to the backbone. The relative peak intensities in the vicinity of  $2\theta = 25^\circ$  are extremely sensitive to the relative stacking (*c*-axis) placement of the two unit cell base chains, nominally at (0,0,0) and (0,  $1/2$ ,  $1/2$ ).

In order to successfully model the observed diffraction features, the following observations are noted:

1. The ratio of the (*h*00) peak intensities can be mimicked using models with only minimal interdigitation (i.e., large side chain tilts) or complete side chain interdigitation.
2. The strength of the (020) reflection requires the average main chain and side chain tilts with respect to the *a*-axis direction to be relatively modest.

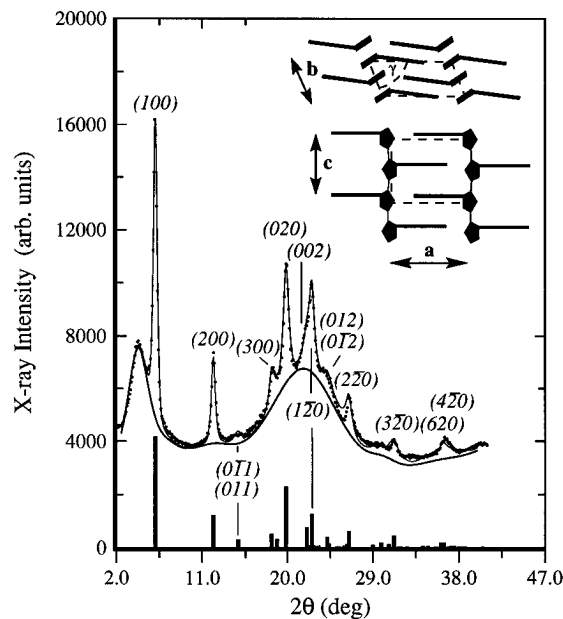


**Figure 2.** Experimental data (dots) and calculated powder diffraction profile (thin line) for P3OT at  $50^\circ \text{C}$  using the type-II structural model schematically shown in the inset. In addition, the explicit (*hk*0) reflections (vertical bars) and the arbitrary background profile (thick solid line) are also shown.

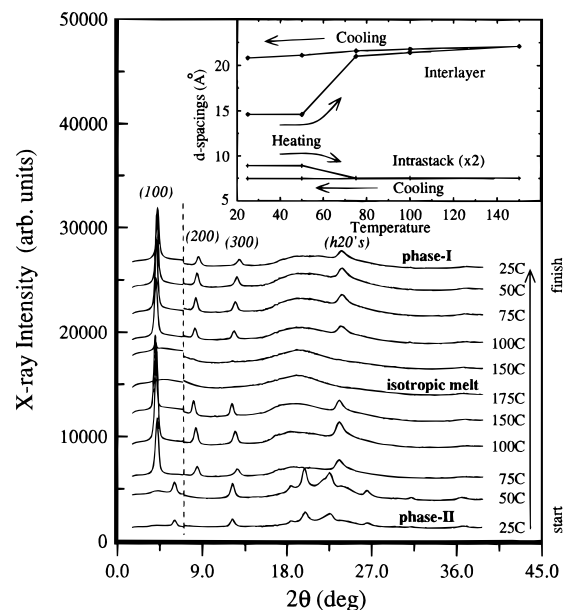


**Figure 3.** X-ray diffraction profiles of R-P3OT at various temperatures demonstrating the solid-state phase change from the type-II to the type-I structure at temperatures well below the isotropic melt. Inset: The measured interlayer and intrastack *d*-spacings of R-P3OT as a function of temperature.

3. The intrastack polythiophene chain-to-chain stacking retains the *d*/2 "out-of-phase" ordering (also seen in IR-P3AT's). This yields the proper peak intensities and positions for scattering features at  $2\theta$  angles higher than the (020) peak. However, some disorder in this stacking is necessary to fully reproduce the shoulder at  $2\theta \sim 24^\circ$  [labeled (012) and (012) in Figure 2]. In this specific case, an eight-chain supercell (or  $b = 37.7 \text{ \AA}$ ) was utilized.

4. The side chains must not exhibit much *a*-*b* plane disorder because this attribute generates large nonzero peak intensities in the  $13\text{--}16^\circ$   $2\theta$  region [labeled (011) and (011) in Figure 2].

The overall structure, in the context of this model, is thus described as having layers of interdigitated, tilted alkyl chains with a 4.47 Å intrastack perpendicular chain-to-chain spacing and a dense average 4.1 Å side chain nearest neighbor spacing. Note that the intrastack chain repeat is a somewhat longer, 4.7 Å (or  $b/2$ ). Similar results (not shown) were also obtained using the P3DDT data ( $a = 19.8$  Å,  $b = 9.37$  Å,  $c = 8.07$  Å, and  $\gamma = 77^\circ$ ). Model calculations based on other possible structures, including those of ref 18, yielded poor agreement with our data. Because of the rather limited interchain  $\pi$ -electron wavefunction overlap arising from the nominal 4.47 Å spacing, this material would be naively expected to have significantly poorer bulk electronic transport properties.

Heating of both R-P3OT and R-P3DDT type-II samples caused them to revert back to the type-I non-ID structural form at temperatures well below those of the isotropic melt (but near temperatures at which the LC phase appears). This transformation can be seen clearly in the R-P3OT thermal cycling data of Figure 3. It is extremely interesting to note that these R-P3AT samples can undergo a direct solid-state transformation from a fully ID state to a non-ID state (and with the associated 30% increase in the interlayer repeat) through only a limited side chain "melting". On cooling from the melt, the conventional type-I structure is recovered. However, if the type-II structure is equivalent to the  $\beta$ -phase reported for R-poly(3-decylthiophene) by Bolognesi et al.,<sup>18</sup> which was obtained by extremely slow cooling from the melt, it is no longer even certain that the common type-I structure is, in fact, the thermodynamically stable one for regioregular P3AT's at room temperature. Additional studies are planned to better address these unusual characteristics.

**Acknowledgment.** The financial support by NSF DMR Grant No. DMR-9305289 (T.J.P. and M.J.W.) and Grant No. CHE-9201198 (R.D.M.) is gratefully acknowledged.

## References and Notes

- (1) Inganäs, O.; Salaneck, W. R.; Österholm, H.; Laakso, J. *Synth. Met.* **1988**, *22*, 395.

- (2) Winokur, M. J.; Spiegel, D.; Kim, Y. H.; Hotta, S.; Heeger, A. J. *Synth. Met.* **1989**, *28*, C419.
- (3) Leclerc, M.; Diaz, F. M.; Wegner, G. *Makromol. Chem.* **1989**, *190*, 3105.
- (4) McCullough, R. D.; Tristram-Nagle, S.; Williams, S. P.; Lowe, R. D.; Jayaraman, M. *J. Am. Chem. Soc.* **1993**, *115*, 4910.
- (5) McCullough, R. D.; Williams, S. P. *J. Am. Chem. Soc.* **1993**, *115*, 11608.
- (6) Chen, T. A.; Wu, X.; Rieke, R. D. *J. Am. Chem. Soc.* **1995**, *117*, 233.
- (7) Rughooputh, S. D. D. V.; Hotta, S.; Heeger, A. J.; Wudl, F. *J. Polym. Sci., Polym. Phys. Ed.* **1987**, *25*, 1071.
- (8) Tashiro, K.; Ono, K.; Minagawa, Y.; Kobayashi, K.; Kawai, T.; Yoshino, K. *J. Polym. Sci., Polym. Phys. Ed.* **1991**, *29*, 1223.
- (9) Prosa, T. J.; Winokur, M. J.; Moulton, J.; Smith, P.; Heeger, A. J. *Macromolecules* **1992**, *25*, 4364.
- (10) *Science and Applications of Conducting Polymers*, Salaneck, W. R., Clark, D. T., Samuelsen, E. J., Eds.; Adam Hilger: Bristol, 1991.
- (11) Mardalen, J.; Samuelsen, E. J.; Gautun, O. R.; Carlsen, P. H. *Synth. Met.* **1992**, *48*, 363.
- (12) Chen, S. A.; Lee, S. T. *Polymer* **1995**, *36*, 1719.
- (13) Tashiro, K.; Kobayashi, K.; Morita, K.; Kawai, T.; Yoshino, K. *Synth. Met.* **1995**, *69*, 397.
- (14) Busing, W. R. *Macromolecules* **1990**, *23*, 4068.
- (15) Brüchner, S.; Porzio, W. *Makromol. Chem.* **1989**, *89*, 961.
- (16) Porzio, W.; Bolognesi, A.; Destri, S.; Catellani, M.; Bajo, B. *Synth. Met.* **1991**, *41*, 537.
- (17) Bolognesi, A.; Catellani, M.; Destri, S.; Porzio, W. *Makromol. Chem., Rapid Commun.* **1991**, *12*, 9.
- (18) Bolognesi, A.; Porzio, W.; Provasoli, F.; Ezquerro, T. *Makromol. Chem.* **1993**, *194*, 817.
- (19) Our data appears to be qualitatively similar to the  $\beta$ -phase poly(3-decylthiophene) of ref 18 but their proposed model is incompatible with this data.
- (20) The "similar"  $\beta$ -phase of Bolognesi et al. is obtained by extremely slow cooling from the isotropic melt.
- (21) McCullough, R. D.; Lowe, R. D.; Jayaraman, M.; Anderson, D. L. *J. Org. Chem.* **1993**, *58*, 904.
- (22) The specific atomic positions are available on request.

MA951510U